

UV absorption cross-sections and atmospheric photolysis lifetimes of halogenated aldehydes

O.V. Rattigan*, O. Wild¹, R.A. Cox

Centre for Atmospheric Science, Department of Chemistry, University of Cambridge, Lensfield Road, Cambridge CB2 1EW, UK

Accepted 8 August 1997

Abstract

UV absorption cross-sections for CCl_3CHO , CCl_2FCHO and CClF_2CHO have been determined over the wavelength range 200–370 nm and at temperatures in the range 298–243 K using a dual beam diode array spectrometer. The spectra show characteristic absorption due to the $n \rightarrow \pi^*$ transition of the C=O group with absorption maxima around 300 nm. On substitution of Cl by F in the CX_3 group the absorption maxima showed a shift to longer wavelengths and a corresponding increase in the intensity of the absorption in the region of atmospheric photolysis. With decreasing temperature, all three aldehydes showed a small non-negligible decrease in the cross-section in the long wavelength tail of the absorption band, and an increase in the cross-section around the absorption maxima. A two-dimensional photochemical model has been used to calculate atmospheric lifetimes due to photodissociation and OH radical loss. © 1998 Elsevier Science S.A.

Keywords: UV absorption cross-section; Atmospheric photolysis; Halogenated aldehydes

1. Introduction

Halogenated aldehydes are produced following the OH-initiated oxidation of hydrofluorocarbons (HFCs) and hydrochlorofluorocarbons (HCFCs) [1] of the type CH_3CX_3 , which are considered as potential replacements for the chlorofluorocarbons (CFCs). The atmospheric removal of these aldehydes can occur in a number of ways including photolysis, reaction with the hydroxyl radical, and uptake into cloud water. Rate data for the reaction of hydroxyl radicals with halogenated aldehydes [2] suggest that increasing halogen substitution decreases the reaction rate constant. Thus compared to acetaldehyde, the atmospheric lifetimes (due to OH attack) of the halogenated aldehydes are considerably longer and are of the order of several days for the chlorinated aldehydes to several weeks for the fluorinated aldehydes. Consequently, other removal processes, e.g., photolysis and aqueous phase uptake may be more competitive.

An accurate knowledge of the absorption cross-section is required in order to estimate the photolysis lifetime. In the troposphere temperatures decrease with increasing altitude;

thus the temperature dependence of the absorption cross-section also needs to be determined.

In this study the absorption cross-sections for CCl_3CHO , CCl_2FCHO and CClF_2CHO were recorded over the wavelength range 200–370 nm and at temperatures from 298 to 243 K, with particular emphasis on the long wavelength tail which is important for atmospheric photolysis. New data are presented for CCl_3CHO which give slightly higher cross-sections in the 220–240 nm region compared to our earlier measurement [3]. The data are compared to other previous measurements [4–6]. Cross-sections for CCl_2FCHO and CClF_2CHO have not been reported previously. Temperature dependent cross-section data have been used in a 2-D atmospheric model to calculate photodissociation lifetimes.

2. Experimental details

Absorption cross-section measurements were made using a 1 m long, jacketed Quartz cell coupled to a dual-beam, diode array spectrometer which has been described in detail previously [3]. The aldehydes were introduced into the sample cell from a Pyrex glass vacuum line fitted with greaseless taps (Young and Co.). Gas pressures were measured with a calibrated capacitance manometer (MKS Baratron, 0–100 Torr model 222 A).

* Corresponding author. Department of Chemistry, Boston College, Chestnut Hill, Boston, MA 02167, USA.

¹ Present address. Earth System Science, University of California, Irvine, CA 92697, USA.

A collimated beam from a 30 W deuterium lamp (Hamamatsu, model L1636) was passed through a beam splitter (Oriel Scientific, model 78150) and the resultant beams were collected in fibre-optic couplers either directly (reference beam) or after passage longitudinally through the cell (sample beam). Both beams were directed, one above the other into the inlet slit of a 275 mm Czerny–Turner spectrograph. A 600 grooves per mm grating with a spectral range of ~ 75 nm was used to disperse the beams over two 512 channel, unintensified silicon diode arrays (Reticon). An entrance slit width of $100 \mu\text{m}$ was used providing a resolution of approximately 0.6 nm (FWHM). With this grating measurements were made over three different spectral regions from 200–370 nm, ensuring at least a 10 nm overlap between adjacent segments. For measurements at wavelengths greater than 300 nm a Pyrex glass filter was mounted in the monitoring beam to prevent higher order radiation from reaching the detector. Wavelength calibrations were made using emission lines of Hg, Zn and Cd from a Philips 93145 Spectral lamp and an entrance slit width of $10 \mu\text{m}$. The accuracy of the wavelength calibration is 0.15 nm . A commercial grade sample of CCl_3CHO was obtained from Fluka with a stated purity of 99%. Samples used for spectral measurements were transferred to a vacuum-tight glass container in a glove box purged with nitrogen in order to exclude water vapour which can lead to hydrate formation. Trap to trap distillation was carried out prior to spectral analysis. CClF_2CHO was prepared on the vacuum line by dehydration of the hydrate $\text{CClF}_2\text{CH}(\text{OH})_2$ (Fluorochem stated purity 97%) with concentrated sulphuric acid [7] and collected at 198 K . The infrared spectrum was in excellent agreement with Yamada et al. [7]. CCl_2FCHO was prepared according to the method of Yamada et al. [8]. Heating the polymerised sample provided a vapour pressure of approximately 3.0 Torr at 298 K sufficient for spectral measurements. The infrared spectra were found to be free of the hydrate.

3. Results

3.1. Room temperature measurements

UV absorption spectra of CCl_3CHO were measured in the wavelength region 200–370 nm and spectra of CCl_2FCHO and CClF_2CHO over the range 235–370 nm at several pressures from 0.20 to 10.0 Torr . Good agreement with the Beer Lambert Law relationship

$$\ln(I_0/I_t) = \sigma Nl \quad (\text{i})$$

was observed at all wavelengths and temperatures, where N is the concentration in molecule cm^{-3} , l is the optical path length in centimeters, σ is the absorption cross-section in centimeter square per molecule and I_0 and I_t are the intensities of the incident and transmitted light beams respectively. Thus the reported cross-sections were obtained by averaging the measurements at several different vapour pressures. In the

Table 1
Absorption cross-sections and temperature coefficients^a for CCl_3CHO

Wavelength (nm)	$\sigma_{298 \text{ K}}$ ($10^{-20} \text{ cm}^2 \text{ molecule}^{-1}$)	B (10^{-4} K^{-1})
200	115.6	8.10
205	86.43	10.2
210	48.19	17.0
215	23.88	25.6
220	10.92	29.1
225	4.730	46.2
230	2.502	53.8
235	1.638	46.6
240	1.425	39.1
245	1.639	31.7
250	2.184	24.2
255	2.934	12.4
260	3.977	2.01
265	5.326	-2.31
270	6.736	-4.95
275	8.128	-5.31
280	9.318	-5.33
285	10.08	-4.53
290	10.32	-4.32
295	9.920	-2.33
300	9.029	-0.20
305	7.672	0.87
310	6.081	4.34
315	4.587	4.33
320	3.066	15.0
325	1.901	13.8
330	1.123	25.9
335	0.498	53.1
340	0.194	88.4
345	0.086	113.2
350	0.020	167.2
355	0.002	235.9
360	0.000	

^aTemperature coefficients (B values) were obtained from a plot of $\ln \sigma_T$ Vs temperature.

overlapping spectral regions the cross-sections were found to agree within approximately 2% (1σ) of each other and were thus averaged to produce the reported cross-sections in Tables 1–3. At wavelengths $< 235 \text{ nm}$ weak transmission of the quartz optical fibres limited the accuracy of the spectral measurements. Thus for CCl_2FCHO and CClF_2CHO which were investigated subsequent to CCl_3CHO , cross-sections at wavelengths $> 235 \text{ nm}$ were recorded. At wavelengths $< 320 \text{ nm}$ the error (1σ) on the cross-sections was typically $\sim 3\%$. Cross-section measurements at longer wavelengths were limited by the baseline drift of ± 0.0005 absorbance units which corresponds to cross-sections of ca. $2 \times 10^{-23} \text{ cm}^2 \text{ molecule}^{-1}$.

Figs. 1–4 show the absorption cross-sections over the wavelength range 200–370 nm. Tabulated values averaged over 5 nm intervals are presented in Tables 1–3.

3.2. Temperature dependence of cross-sections

Absorption measurements were also made at several temperatures in the range 298–243 K. At each temperature at

Table 2
Absorption cross-sections and temperature coefficients for CCl_2FCHO

Wavelength (nm)	$\sigma_{298\text{ K}}$ ($10^{-20} \text{ cm}^2 \text{ molecule}^{-1}$)	B (10^{-4} K^{-1})
235	0.402	136.0
240	0.502	87.0
245	1.080	30.6
250	1.597	6.41
255	2.391	1.24
260	3.483	-6.12
265	4.869	-7.55
270	6.527	-8.11
275	8.351	-8.28
280	10.12	-8.04
285	11.75	-7.82
290	12.96	-6.89
295	13.70	-6.41
300	13.60	-4.50
305	12.91	-2.93
310	11.60	1.73
315	9.803	2.70
320	7.927	6.97
325	5.614	12.2
330	3.889	15.6
335	2.457	24.6
340	1.260	36.5
345	0.628	58.1
350	0.254	84.9
355	0.052	92.8
360	0.017	93.2
365	0.007	103.2
370	0.002	138.3

Table 3
Absorption cross-sections and temperature coefficients for CClF_2CHO

Wavelength (nm)	$\sigma_{298\text{ K}}$ ($10^{-20} \text{ cm}^2 \text{ molecule}^{-1}$)	B (10^{-4} K^{-1})
235	0.192	-29.0
240	0.408	-17.9
245	0.736	-13.5
250	1.246	-11.8
255	1.992	-10.7
260	3.018	-10.5
265	4.357	-10.4
270	6.052	-10.5
275	8.001	-9.96
280	10.09	-10.6
285	12.12	-10.2
290	14.02	-10.6
295	15.38	-9.54
300	16.26	-10.4
305	15.93	-7.09
310	15.43	-9.73
315	13.36	-8.32
320	11.70	-7.71
325	9.284	-5.02
330	6.581	-3.03
335	4.759	-2.83
340	2.842	-2.84
345	1.516	14.0
350	0.711	37.3
355	0.148	68.1
360	0.036	75.8
365	0.012	52.9
370	0.003	63.1

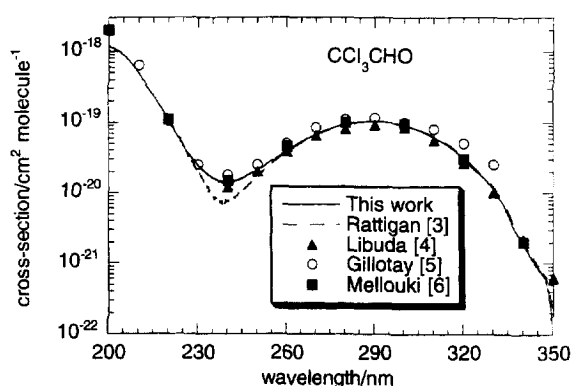


Fig. 1. Absorption cross-sections for CCl_3CHO at 298 K determined in this work (solid line), Rattigan et al. [3] (dashed line), Libuda et al. [4] (filled triangles), Gillotay et al. [5] (open circles), and Mellouki et al. [6] (filled squares).

least five spectra were recorded over a range of pressures and the data averaged to produce the absorption cross-section at that temperature. The spectra illustrated in Figs. (2)–(4) show a decline in the cross-section in the long wavelength tail of the absorption band, at wavelengths > 330 nm, and a corresponding increase in the cross-section around the band maxima with decreasing temperature. The standard deviation on the absolute values for CCl_3CHO at 243 K were approx-

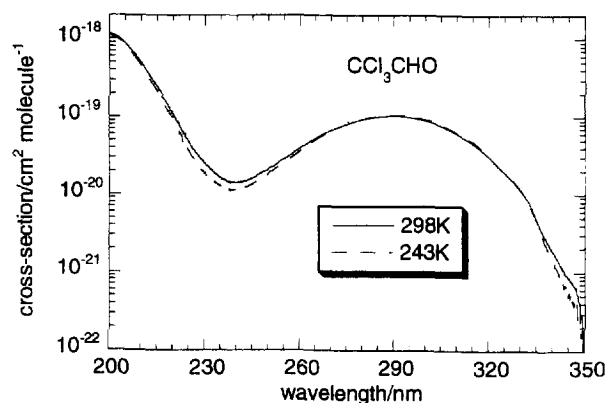


Fig. 2. Absorption cross-sections for CCl_3CHO at 298 and 243 K.

imately 5% for wavelengths < 330 nm increasing to 50% near 355 nm.

4. Discussion

The halogenated acetaldehydes show characteristic absorption in the wavelength region 240–340 nm with band maxima around 290 nm which is attributed to the $n \rightarrow \pi^*$ transition of the carbonyl group. However, it appears that substitution of Cl by F causes the band centre to be red shifted

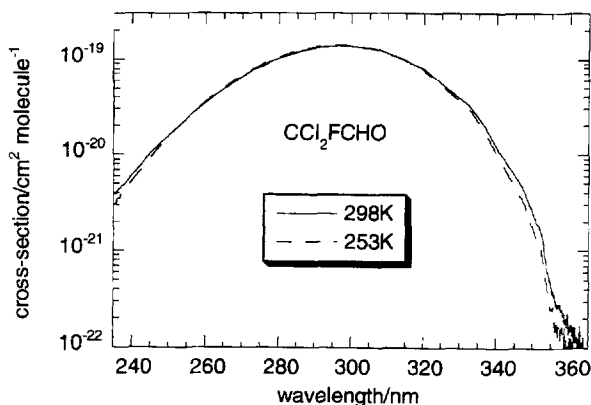


Fig. 3. Absorption cross-sections for CCl_2FCHO at 298 and 253 K.

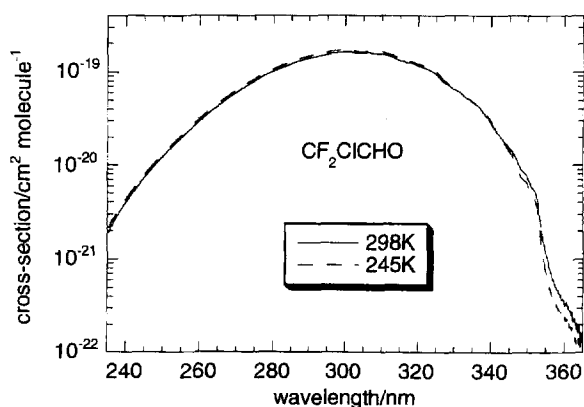


Fig. 4. Absorption cross-sections for CClF_2CHO at 298 and 245 K.

with a corresponding increase in intensity of σ_{max} . Thus for CCl_3CHO the $n \rightarrow \pi^*$ band has a maximum around 289 nm ($\sigma = 10.4 \times 10^{-20} \text{ cm}^2 \text{ molecule}^{-1}$), in CCl_2FCHO the band centre is near 296 nm ($\sigma = 13.8 \times 10^{-20} \text{ cm}^2 \text{ molecule}^{-1}$) and in CClF_2CHO the band maximum is at 300 nm ($\sigma = 16.5 \times 10^{-20} \text{ cm}^2 \text{ molecule}^{-1}$). This is in contrast to the formyl halides, HCOF and HCOCl ; there a blue shift is observed on going from HCOCl , which has an absorption maximum at 260 nm [9], to HCOF whose absorption maximum appears at 210 nm [10].

4.1. Room temperature

The room temperature absorption cross-section for CCl_3CHO has been previously determined by Libuda et al. [4], Gillotay et al. [5] and Mellouki et al. [6]. Within the experimental uncertainties all of the data are in good agreement throughout most of the wavelength range as shown in Fig. 1. Our previous data [3] gave somewhat lower values in the region 220–240 nm. Low light transmission by the optical fibres is a major limitation at wavelengths < 240 nm. At wavelengths > 300 nm the data of Gillotay et al. [5] appears somewhat higher than the average; the difference being greater than a factor of 2 at 330 nm.

There are no previous measurements of the absorption cross-sections for CCl_2FCHO and CClF_2CHO with which to

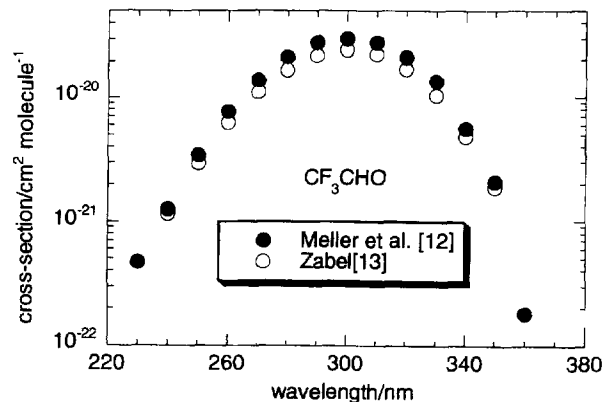


Fig. 5. Absorption cross-section of CF_3CHO at 298 K determined by Meller et al. [12] filled circles and Zabel (footnote 2) open circles.

compare. The absorption spectra are typical of acetaldehydes with absorption cross-sections of $13.8 \times 10^{-20} \text{ cm}^2 \text{ molecule}^{-1}$ and $16.5 \times 10^{-20} \text{ cm}^2 \text{ molecule}^{-1}$ at the absorption maxima respectively. CClF_2CHO shows weak structure similar to that observed in the absorption spectrum of CH_3CHO [11]. Meller et al. [12] have determined the room temperature cross-section for CF_3CHO . The magnitude of the absorption cross-section is approximately a factor of 3 lower than that for CCl_3CHO with a maximum cross-section of approximately $3.03 \times 10^{-20} \text{ cm}^2 \text{ molecule}^{-1}$ around 301 nm. Zabel² also measured the cross-section for CF_3CHO at 298 K. Although there is good agreement in the general shape of the spectrum between the two groups, as shown in Fig. 5, the data obtained by Zabel (footnote 2) are lower than those of Meller et al. [12] by approximately 25% throughout the entire wavelength range. A small systematic error in the estimation of the aldehyde concentration by one of the groups could account for the discrepancy in the reported cross-section.

4.2. Temperature dependences

CCl_3CHO , CCl_2FCHO and CClF_2CHO showed a distinct variation in the absorption cross-section with temperature, see Figs. (2)–(4) (the temperature dependence of CF_3CHO has not been determined). A decrease in the cross-section was observed in the long wavelength wings of the absorption bands and an increase at the band maxima was observed with declining temperatures. The temperature dependence of the absorption cross-section for CCl_3CHO has also been investigated by Gillotay et al. [5] and Mellouki et al. [6]. The magnitude of the temperature dependence is similar to that observed here. For the purposes of parameterising the data the best fit to the temperature dependence for the halogenated aldehydes was obtained by plotting the data in the form $\ln \sigma$ vs temperature. We used this relationship earlier in the temperature dependent parameterization of the broad continuous absorption spectra of the halogenated carbonyl type com-

² F. Zabel, personal communication.

pounds [3]. A typical plot illustrating the temperature dependence of the cross-section for CCl_3CHO for selected wavelengths > 330 nm is shown in Fig. 6. The temperature coefficients obtained from the slope of the plots using a linear least squares analysis routine are listed together with the room temperature cross-sections for CCl_3CHO in Table 1. Tables 2 and 3 show the corresponding recommended temperature coefficient data for CCl_2FCHO and CClF_2CHO . Thus, for the purpose of atmospheric modelling the cross-sections at any temperature can be calculated using the following expression:

$$\ln \sigma_T = \ln \sigma_{298} + B[T - 298] \quad (\text{ii})$$

where σ_T and σ_{298} are the absorption cross-sections at a wavelength, λ , and at temperatures T and 298 K, respectively, and B is the temperature coefficient or gradient. This expression was found to reproduce the measured cross-sections at all temperatures to within ca. 3%. The variation in the cross-section with temperature can be rationalized in terms of a change in the Boltzmann population of the vibrational and rotational levels of the ground electronic state of the molecules at the lower temperatures [13].

4.3. Atmospheric modelling

Atmospheric photolysis rates of the halogenated aldehydes CCl_3CHO , CCl_2FCHO , CClF_2CHO were calculated using the absorption cross-sections shown in Tables 1–3. For CF_3CHO absorption cross-sections of Meller et al. [12] were used. These calculations were carried out using the Cambridge two dimensional model which has been described in detail elsewhere [14]. Atmospheric conditions appropriate to a Northern Hemisphere Spring were used. Photodissociation rate coefficients (J values) were obtained by integrating the product of the absorption cross-section, σ , and the solar flux intensity, F , over the absorbing wavelength range, λ :

$$J = \int \sigma_T(\lambda) \Phi(\lambda) F(\lambda) d\lambda \quad (\text{iii})$$

In these calculations temperature dependent cross-sections reported in Tables 1–3 were used assuming a quantum efficiency (Φ) of unity for the photodissociative process:



Thus the J values presented in Fig. 7 at 30°N represent upper limits. In general fast photolysis rates are observed with tropospheric values varying from $0.7 \times 10^{-4} \text{ s}^{-1}$ for CCl_3CHO and CF_3CHO to $0.4 \times 10^{-3} \text{ s}^{-1}$ for CClF_2CHO (CCl_2FCHO having an intermediate value of near $0.2 \times 10^{-3} \text{ s}^{-1}$). J values remain fairly uniform from the surface to about 20 km thereafter showing a small increase with altitude (values at 50 km are about a factor of two larger). Table 4 shows calculated lifetimes due to photolysis and reaction with the OH radical for the halogenated aldehydes (acetaldehyde is shown for comparison) using conditions appropriate to 30°N and 8.75 km. These values are diurnal averages.

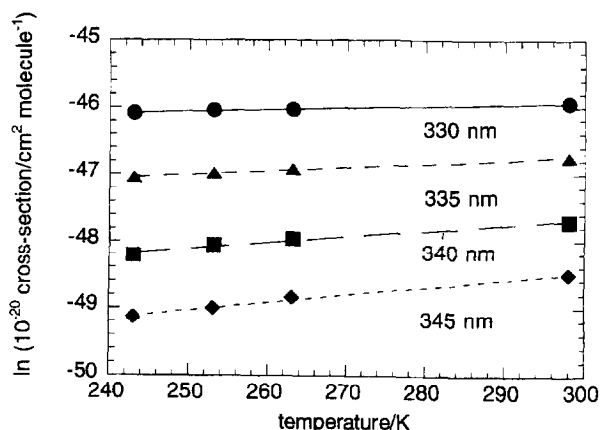


Fig. 6. Logarithm of the absorption cross-section vs. temperature for selected wavelengths in the near ultraviolet tail of the absorption band for CCl_3CHO . The lines show least squares fits to the data.

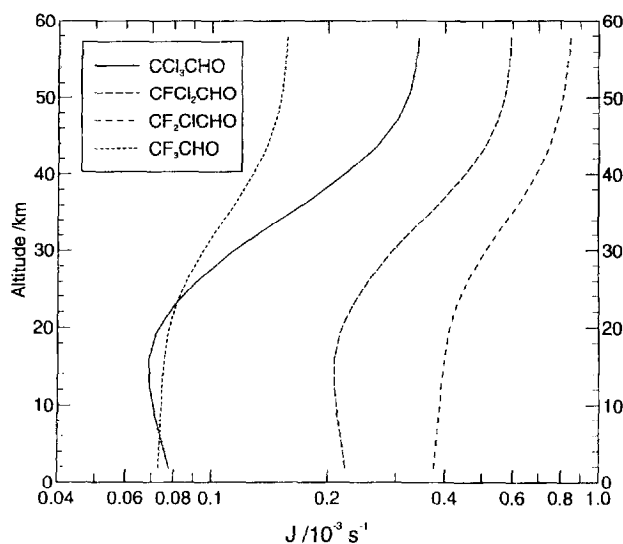


Fig. 7. Calculated J values (s^{-1}) for the halogenated aldehydes as a function of altitude (km) for conditions appropriate to 30°N in spring. A photodecomposition quantum yield of unity was assumed.

Table 4
Lifetimes in hours due to photolysis and reaction with OH

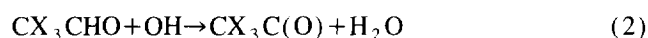
Aldehyde	Photolysis	OH
CH_3CHO	10	17
CCl_3CHO	4	130
CCl_2FCHO	1.3	200
CClF_2CHO	1	270
CF_3CHO	4 ^a	500

Calculations were carried out using the Cambridge 2-D model [14] for conditions appropriate to 30°N and 8.75 km. A photodissociation quantum efficiency of unity was assumed. ^aAbsorption cross-sections from Meller et al. [12] were used.

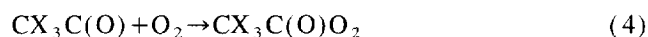
The results of the model calculations in Table 4 show that photolysis is the major removal process for the halogenated aldehydes in the troposphere; for example the photolysis lifetime for CCl_3CHO is approximately 4 h compared to approx-

imately 5 days for removal by the OH radical. In the case of the fluorinated aldehydes CCl_2FCHO and CClF_2CHO photolysis is at least two orders of magnitude faster than reaction with the OH radical. This is in contrast to CH_3CHO where photolysis and reaction with the OH radical are competitive processes. These results indicate that in the troposphere the halogenated aldehydes CCl_3CHO , CCl_2FCHO , CClF_2CHO and CF_3CHO produced from the OH-initiated photo-oxidation of HCFCs and HFCs will be removed close to their source regions. Therefore they are not expected to accumulate in significant amounts [15].

Reaction of the aldehydes with OH radicals occurs via abstraction of the aldehydic H atom to form the acetyl radical $\text{CX}_3\text{C}(\text{O})$ reaction (Eq. (2)):

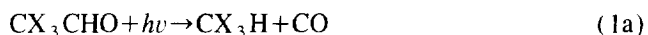


Subsequently, the $\text{CX}_3\text{C}(\text{O})$ radical may either undergo unimolecular decomposition to $\text{CX}_3 + \text{CO}$ or react with O_2 leading to $\text{CX}_3\text{C}(\text{O})\text{O}_2$ formation:



Decomposition is favoured when $\text{X} = \text{Cl}$, whereas when $\text{X} = \text{F}$ addition of O_2 predominates [16]. Under normal atmospheric conditions reaction of $\text{CX}_3\text{C}(\text{O})\text{O}_2$ with NO will lead to CX_3CO_2 which subsequently decomposes to CX_3 and CO_2 . Under a high NO_2 regime as commonly found close to urban and industrial emission regions however, the corresponding acetylperoxynitrate, $\text{CX}_3\text{C}(\text{O})\text{O}_2\text{NO}_2$, may be formed. These peroxynitrates will be in thermal equilibrium with their precursors $\text{CX}_3\text{C}(\text{O})\text{O}_2$ and NO_2 . Close to the surface thermal decomposition will predominate whereas at temperatures corresponding to the upper troposphere they have been shown to be very stable [16,17]. Under these conditions they could therefore act as temporary halogen and NO_x reservoirs.

In the case of photolysis the following four channels (Eqs. (1a)–(1d)) need to be considered:



Pathway (1a) will lead to the halogenated methane type species (CCl_3H , Cl_2FH and ClF_2H) which are much more stable to photodecomposition in the troposphere than the original aldehyde. If formed these species could potentially be transported in small amounts to the lower stratosphere with subsequent photodegradative release of the bound halogen atoms. In (1b) a halogenated methyl radical, CX_3 , is formed and further oxidation will produce the carbonyl halides, COX_2 , whose likely tropospheric fate is aqueous phase hydrolysis [18]. Photodecomposition via pathway (1c) leads to the formation of the corresponding halogenated acyl

radical $\text{CX}_3\text{C}(\text{O})$ as in Eq. (2) above. Cleavage of a CCl bond, pathway (1d), will lead to CX_2CHO which will decompose to CX_2 and CHO and on further oxidation lead to CX_2O and CO_2 . Information on the photodissociation mechanism of the halogenated aldehydes is rather limited [19].^{3,4} Very low yields (1–2%) of H atoms were measured using resonance fluorescence following pulsed laser photolysis of CCl_3CHO at 193, 248 and 308 nm (footnote 3). However, unit quantum yields of Cl atoms were observed. In a static system C_2Cl_6 , CHCl_3 and CO were observed as products from the photolysis of CCl_3CHO at 248 nm (footnote 4). Richer et al. [19] observed production of CF_3H , COF_2 , CO and CO_2 in the 254 nm photolysis of CF_3CHO . The authors proposed pathways (1a) and (1b) to explain their results. These studies would indicate that formation of $\text{CX}_3\text{C}(\text{O})$ (pathway (1c)) is a minor process in the photolysis of halogenated aldehydes. However, secondary chemistry may add complications to these photodissociation mechanisms particularly in static systems. The quantum yields of the various channels so far remain undetermined. Photodissociation of CClF_2CHO and CCl_2FCHO has not been investigated. Clearly, further work is required in order to fully access the importance of species such as CX_3H and $\text{CX}_3\text{C}(\text{O})\text{O}_2\text{NO}_2$ as temporary halogen and/or NO_x reservoirs.

5. Conclusions

The UV absorption cross-sections of the halogenated aldehydes CCl_3CHO , CCl_2FCHO and CClF_2CHO have been determined over the wavelength range 200–370 nm and for temperatures from 298 to 243 K. A two-dimensional model has been used to calculate atmospheric lifetimes due to photodecomposition and reaction with OH radicals. Relatively short photolysis lifetimes of the order of hours were calculated for all of the aldehydes whereas the OH lifetimes were several days. Thus halogenated acetaldehydes formed from the OH initiated oxidation of HCFCs and HFCs in the atmosphere will be removed near to their sources. Following their photodecomposition small amounts CX_3H and acetylperoxy nitrates ($\text{CX}_3\text{C}(\text{O})\text{O}_2\text{NO}_2$) may be formed which may act as temporary halogen or NO_x reservoirs. Further research on the photodecomposition of the halogenated aldehydes is required to fully assess the importance of these reservoirs.

Acknowledgements

This work was funded by the Alternative Fluorocarbon Environment Acceptability Study SPA-AFEAS, INC under contract P90-007 and the UK Department of the Environment

³ R. Talukdar, personal communication.

⁴ A. Mellouki, personal communication.

on contract PECD 7/12/47. Thanks to D. Scollard, University College Dublin for providing the sample of CCl_2FCHO .

References

- [1] Scientific Assessment of Stratospheric Ozone, World Meteorological Organisation Report No. 20, Vol. 2, 1989.
- [2] D.J. Scollard, J.J. Treacy, H.W. Sidebottom, C. Balestra-Garcia, G. Laverdet, G. LeBras, H. MacLeod, S. Teton, *J. Phys. Chem.* 97 (1993) 4683.
- [3] O.V. Rattigan, O. Wild, R.L. Jones, R.A. Cox, *J. Photochem. Photobiol. A: Chem.* 76 (1993) 1.
- [4] H.G. Libuda, F. Zabel, K.H. Becker, UV spectra of some organic chlorine and bromine compounds of atmospheric interest, STEP-HALOCSIDE/AFEAS Workshop, Dublin, May 1991, University College Dublin.
- [5] D. Gillotay, P.C. Simon, L. Dierickx, UV absorption cross-sections of some carbonyl compounds and their temperature dependence, Quadrennial Ozone Symposium, University of Virginia, June 1992.
- [6] A. Mellouki, R. Talukdar, J.B. Burkholder, G. Le Bras, A.R. Ravishankara, Low Temperature Chemistry of the Atmosphere, NATO Advanced Study Institute, Maratea, August 1993.
- [7] B. Yamada, R.W. Campbell, O. Vogl, *J. Polym. Sci.* 15 (1977) 1123.
- [8] B. Yamada, R.W. Campbell, O. Vogl, *Polym. J.* 9 (1977) 23.
- [9] H.G. Libuda, F. Zabel, E.H. Fink, K.H. Becker, *J. Phys. Chem.* 94 (1990) 5860.
- [10] L.E. Jr. Giddings, K.K. Innes, *J. Mol. Spectrosc.* 6 (1961) 528.
- [11] R. Atkinson, D.L. Baulch, R.A. Cox, R.F. Jr. Hampson, J.A. Kerr, J. Troc, *J. Phys. Chem. Ref. Data* 18 (1989) 881.
- [12] R. Meller, D. Boglu, G.K. Moortgat, Absorption cross-sections and photolysis studies of halogenated carbonyl compounds, Photooxidation studies on CF_3 -containing CFC-substitutes, STEP-HALOCSIDE/AFEAS Workshop, Dublin, March 1993, University College Dublin.
- [13] H. Okabe, *Photochemistry of Small Molecules*, Wiley, New York, 1978.
- [14] K.S. Law, J.A. Pyle, *J. Geophys. Res.* 98 (1993) 18377.
- [15] O. Wild, O.V. Rattigan, R.L. Jones, J.A. Pyle, R.A. Cox, *J. Atmos. Chem.* 25 (1996) 167.
- [16] I. Barnes, K.H. Becker, F. Kirchner, F. Zabel, Formation and thermal decomposition of $\text{CCl}_3\text{C}(\text{O})\text{O}_2\text{NO}_2$ and $\text{CF}_3\text{C}(\text{O})\text{O}_2\text{NO}_2$, STEP-HALOCSIDE/AFEAS Workshop, Dublin, March 1993 University College Dublin.
- [17] F. Zabel, F. Kirchner, K.H. Becker, *Int. J. Chem. Kinet.* 26 (1994) 827.
- [18] W.J. DeBruyn, S.X. Duan, X.Q. Shi, P. Davidovits, D.R. Worsnop, M.S. Zahniser, C.E. Kolb, *Geophys. Res. Lett.* 19 (1992) 1939.
- [19] H.R. Richer, J.R. Sodeau, I. Barnes, The photolysis and chlorine-initiated photooxidation of trifluoroacetaldehyde, STEP-HALOCSIDE/AFEAS Workshop, Dublin, March, 1993, University College Dublin.